Journal of Hydrology 554 (2017) 317–330

Contents lists available at ScienceDirect

Journal of Hydrology

journal homepage: www.elsevier.com/locate/jhydrol

Research papers

Use of a scenario-neutral approach to identify the key hydro-meteorological attributes that impact runoff from a natural catchment

Danlu Guo *, Seth Westra, Holger R. Maier

School of Civil, Environmental and Mining Engineering, The University of Adelaide, North Terrace, Adelaide SA 5000, Australia

ARTICLE INFO

Article history:
Received 17 January 2017
Received in revised form 3 June 2017
Accepted 12 September 2017
Available online 18 September 2017
This manuscript was handled by A. Bardossy, Editor-in-Chief

Keywords:
Scenario-neutral
Climate impact study
Inverse approach
Stochastic generator
Climate exposure space
Sensitivity analysis

ABSTRACT

Scenario-neutral approaches are being used increasingly for assessing the potential impact of climate change on water resource systems, as these approaches allow the performance of these systems to be evaluated independently of climate change projections. However, practical implementations of these approaches are still scarce, with a key limitation being the difficulty of generating a range of plausible future time series of hydro-meteorological data. In this study we apply a recently developed inverse stochastic generation approach to support the scenario-neutral analysis, and thus identify the key hydro-meteorological variables to which the system is most sensitive. The stochastic generator simulates synthetic hydro-meteorological time series that represent plausible future changes in (1) the average, extremes and seasonal patterns of rainfall; and (2) the average values of temperature (T_a), relative humidity (RH) and wind speed (u_z) as variables that drive PET. These hydro-meteorological time series are then fed through a conceptual rainfall-runoff model to simulate the potential changes in runoff as a function of changes in the hydro-meteorological variables, and runoff sensitivity is assessed with both correlation and Sobol' sensitivity analyses. The method was applied to a case study catchment in South Australia, and the results showed that the most important hydro-meteorological attributes for runoff were winter rainfall followed by the annual average rainfall, while the PET-related meteorological variables had comparatively little impact. The high importance of winter rainfall can be related to the winter-dominated nature of both the rainfall and runoff regimes in this catchment. The approach illustrated in this study can greatly enhance our understanding of the key hydro-meteorological attributes and processes that are likely to drive catchment runoff under a changing climate, thus enabling the design of tailored climate impact assessments to specific water resource systems.

1. Introduction

Scenario-neutral approaches are being used increasingly to assess the potential impact of climate change on the performance of water resources systems (Brown et al., 2012; Brown and Wilby, 2012; Dessai and Hulme, 2004; Nazemi and Wheater, 2014). These approaches provide useful information for assessing system vulnerability under alternative climate change scenarios, and for defining climatic thresholds at which system performance begins to change abruptly (Brown et al., 2011; Poff et al., 2015). Another unique feature of scenario-neutral approaches is their ability to identify the hydro-meteorological variables that have the greatest impact on the specific water resource system under consideration. This feature is particularly useful to provide guidance for selecting: (1) climate models; (2) strategies to generate fine-scale future rainfall and climate conditions from GCM-based projections (known as statistical downscaling); and/or (3) alternative 'lines of evidence' (e.g. expert opinion and data from the paleo-climatic record) that can provide useful information about the future changes in these key variables (Prudhomme et al., 2002; Vano et al., 2015; Wilcke and Bärring, 2016). Ultimately, scenario-neutral approaches can support the development of a more complete set of climate projections that describe how the key variables might change in a greenhouse gas-enhanced climate (Nazemi et al., 2013; Singh et al., 2014; Steinschneider and Brown, 2013; Vano et al., 2015).

Although the general principles underpinning scenario-neutral approaches have been well established (Brown et al., 2012; Dessai and Hulme, 2004; Nazemi and Wheater, 2014; Prudhomme et al., 2010), practical implementations have only appeared in the literature relatively recently (Brown et al., 2012; Culley et al., 2016; Kay et al., 2014; Poff et al., 2015; Prudhomme et al., 2013, 2010; Singh et al., 2014). A key challenge in the

* Corresponding author.
E-mail address: Danlu.Guo@Adelaide.edu.au (D. Guo).

http://dx.doi.org/10.1016/j.jhydrol.2017.09.021
0022-1694/

implementation of scenario-neutral approaches is the generation of a set of plausible climate conditions (referred to as the 'exposure space'; see Culley et al., 2016) to which a system might be exposed in the future. Ideally, this exposure space should consider a range of possible variations not only in the average states of the relevant hydro-meteorological variables, such as annual average rainfall and potential evapotranspiration (see Kay et al., 2014; Prudhomme et al., 2013), but also a number of other attributes for each variable, including extremes, seasonality and inter-annual variability (Meselhe et al., 2009; Moody and Brown, 2013; Prudhomme et al., 2010; Steinschneider and Brown, 2013). In this way, the sensitivity of water resource systems can be tested against a comprehensive range of potential climate changes that can be expected in a greenhouse gas-enhanced climate (Prudhomme et al., 2013; Steinschneider and Brown, 2013).

Despite the benefits of considering a wide range of hydro-meteorological variables and a variety of their attributes, in most previous scenario-neutral studies, climate exposure spaces have been produced with perturbations on a small number of hydro-meteorological variables. In particular, most studies have relied on perturbing annual and/or monthly average rainfall and potential evapotranspiration through the use of simple scaling factors (Kay et al., 2014; Paton et al., 2013; Prudhomme et al., 2013, 2010; Singh et al., 2014). To expand the applicability of scenario-neutral approaches to investigate the implications of changes not only to the averages but also to other attributes of the hydro-meteorological variables of interest, the use of stochastic generators has been proposed. This has been illustrated in Whateley et al. (2014), in which the parameters of a weather generator were perturbed, followed by quantile correction of the generated time series, to achieve a set of pre-specified 'target' levels of climate statistics. A challenge with this approach, however, arises with the difficulty to assess *a priori* which parameters of the stochastic generator should be modified to produce hydro-meteorological time series that represent the different target statistics. This, in turn, potentially leads to insufficient exploration of the exposure space, and the associated risk that key modes of system vulnerability are not explored as part of the scenario-neutral analysis.

A potential way to address this issue was proposed by Guo et al. (2016a), who developed an 'inverse' approach to enable stochastic generation of time series that represent pre-specified changes of each hydro-meteorological variable of interest. In this way, the inverse approach enables a range of plausible future climate conditions to be explored, and thus can be used to provide uniform coverage of the exposure space and to serve the needs of comprehensive scenario-neutral climate impact assessments. Although the approach is in principle applicable to perturb any hydro-meteorological variable(s) that can be generated by parametric stochastic generators, Guo et al. (2016a) focused only on perturbing four attributes of rainfall (i.e. average daily rainfall, annual wet days, average dry-spell length and the 99th percentile of daily rainfall). Furthermore, the approach has not yet been utilized as part of a formal application of the scenario-neutral approach.

Therefore, this study aims to extend the applicability of the inverse approach of Guo et al. (2016a) to a wider set of hydro-meteorological variables and their statistics (collectively referred to as 'hydro-meteorological attributes'), and to apply the synthetic hydro-meteorological time series to test the climate sensitivity of a water resource system. To demonstrate the approach, six attributes that are likely to affect catchment runoff are identified *a priori* based on system understanding, and a formal correlation and a Sobol' sensitivity analyses are subsequently applied to identify which of these attributes have the greatest impact on several runoff indices of interest. In doing so, this study greatly expands the applicability of scenario-neutral approaches to a wider range of possible climatic changes, while still focusing the analysis on those attributes that are most relevant for the specific system.

The subsequent sections of this paper are structured as follows. Section 2 introduces the case study catchment and data used to illustrate the scenario-neutral approach. Section 3 describes the methodology used to implement the scenario-neutral approach to identify the key hydro-meteorological attributes for the case study catchment, including a description of (i) the generation of climate exposure spaces with the inverse approach; followed by (ii) a climate stress test on the catchment runoff. Section 4 presents and discusses two sets of results regarding (i) the performance of the inverse approach in terms of its ability to generate the desired climate exposure space; and (ii) the key hydro-meteorological attributes identified to have high impact on catchment runoff. Section 5 discusses the links between the study results to understanding of the specific case study, as well as the study limitations and future work required for designing a more comprehensive scenario-neutral application. The study is summarized and concluded in Section 6.

2. Case study and data

We focused on a case study for the Scott Creek catchment, which is a small (29 km^2) catchment located in the southern Mount Lofty Ranges close to Adelaide, South Australia. This catchment was selected as it has been well-studied, is highly sensitive to climatic changes and has minimal anthropogenic modifications (Westra et al., 2014a). The catchment has mean annual rainfall of 892 mm and PET of 1372 mm over the study period from 1995 to 2004. The climate is classified as Mediterranean, exhibiting a winter-dominated rainfall regime with over 75% of the rainfall occurring within the period from July to September (winter and early spring) in an average year. Furthermore, the distribution of runoff is highly skewed, with approximately 30% of the total flow volume contributed from the top 1% of flow days (Westra et al., 2014a).

As part of the scenario-neutral approach, a number of relevant hydro-meteorological attributes need to be selected to construct the climate exposure space (Prudhomme et al., 2013), and these attributes are then run through a hydrological model to assess the implications of changes in each attribute on hydrological response. The emphasis of this study is to assess a larger number of hydro-meteorological attributes than those commonly considered for scenario-neutral studies, and as such, we focused on six hydro-meteorological attributes that could be expected to influence overall catchment response (Table 1). The selection of these attributes were based on *a priori* understanding of catchment function of the case study (e.g. Westra et al., 2014a), so that they represent the hydro-meteorological characteristics deemed most likely to impact upon runoff in this region. In particular, to

Table 1
Definitions and baseline values of the six hydro-meteorological attributes included in the exposure space.

Hydro-meteorological attribute	Definition	Average baseline value (1995–2004)
PD	Daily rainfall intensity averaged over all wet days	6.38 mm/day
Pex99	99th percentile of daily rainfall over wet days	40.0 mm/day
PJJA	Daily rainfall intensity averaged over winter (June, July and August)	7.28 mm/day
T_a	Daily average temperature	17.0 °C
RH	Daily average relative humidity	61.2%
u_z	Daily average wind speed	3.16 m·s^{-1}

represent changes to rainfall patterns, we focused on variations in the average wet-day rainfall (*PD*) as a measure of average rainfall, and the 99th percentile of wet-day rainfall (*Pex99*) as a measure of extreme rainfall. Both rainfall attributes are closely related to the detection and attribution of climate change, as described by the Expert Team on Climate Change Detection and Indices (ETCCDI) (Klein Tank et al., 2009). In addition, winter rainfall (*PJJA*) was also considered, since a large portion of catchment runoff occurs during this season. Although potential changes in hydro-meteorological variables are usually assumed to influence catchment response via changes to the driving variables of rainfall and PET, it was shown that the manner in which PET is perturbed (and in particular, the meteorological variable used to perturb PET) can have a significant impact on runoff (Guo et al., 2016c). As such, rather than directly modifying PET, we analyzed the effects of changing daily average temperature (T_a), relative humidity (*RH*) and wind speed (u_z), which were identified as the key driving variables for PET at the case study location (Guo et al., 2016c). The conversion from potential changes in these driving variables to PET was undertaken using the Penman-Monteith model.

The response of catchment runoff to changes in the various hydro-meteorological attributes was then assessed using the conceptual rainfall-runoff model GR4J, as it has been shown to provide a good representation of underlying physical processes for the case study catchment (Guo et al., 2017; Westra et al., 2014a). To calibrate the model, historical rainfall and runoff data were obtained at the case study catchment. The PET data were estimated using the Penman-Monteith model with historical climate data of temperature, relative humidity, solar radiation and wind speed, using the R package *Evapotranspiration* (http://cran.r-project.org/web/packages/Evapotranspiration/index.html) (Guo et al., 2016b). Since over 80% of the catchment area is covered by grass (Evans and Jakeman, 1998), the evaporative surface for the entire catchment was assumed to be the reference crop, enabling the FAO-56 version of the Penman-Monteith model (Allen et al., 1998) to be used. The data sources are detailed as below:

1. **Catchment-average rainfall (mm)**: Since the catchment is relatively small, daily rainfall data were obtained from a rain gauge within the catchment (Australian Bureau of Meteorology gauge number: 23727) and assumed to represent the catchment-average rainfall.
2. **Daily maximum and minimum temperature (T_{max} *and* T_{min} in °C), maximum and minimum relative humidity (RH_{max} *and* RH_{min} in %) and wind speed (u_z in m/s):** Due to the limited availability of high-quality climate data, data on each of these variables were obtained directly from the Kent Town weather station, which is located approximately 20 km from the catchment outlet.
3. **Daily solar radiation (R_s in MJ/(m^2.day)):** Daily solar radiation was calculated from daily sunshine hour data (n in hrs) obtained from the Kent Town weather station, using the Ångström-Prescott equation (McMahon et al., 2013), with constants provided in Chiew and McMahon (1991).
4. **Catchment runoff (ML/day)**: Daily runoff data were obtained from the gauging stations at the outlet of Scott Creek catchment, and were then converted to mm to represent the catchment-average runoff for each day.

With the abovementioned data, GR4J was calibrated following a 70:30 split-sample calibration (Klemeš, 1986), which led to a calibration period from 1995 to 2001, and a validation period between 2002 and 2004. The model illustrated satisfactory performance for both the calibration (NSE of 0.873; relative bias of 0.007) and validation (NSE of 0.855; relative bias of 0.009) periods. In addition to calibrating the rainfall-runoff model, the climate data from the combined calibration and validation period were used as a baseline to produce synthetic hydro-meteorological time series that covered the climate exposure space (baseline values given in Table 1).

Table 2
Definitions and baseline values of the five runoff attributes selected to represent the runoff response for the case study catchment.

Runoff attribute	Definition	Average baseline value
Qavg	Daily average runoff over all days	0.367 mm
Q99	99th percentile of daily runoff over all days	5.014 mm
Q10	10th percentile of daily runoff over all days	0.006 mm
QJJA	Daily runoff averaged over winter (June, July and August)	0.912 mm
QSON	Daily runoff averaged over spring (September, October and November)	0.464 mm

To assess the sensitivity of runoff with the scenario-neutral approach, we focused on five key attributes representing different features of runoff for the Scott Creek catchment. These include: the average daily runoff for all days (*Qavg*), a measure of peak flow as the 99th percentile of daily runoff (*Q99*), a measure of low flow as the 10th percentile of daily runoff (*Q10*), and the average daily runoff for winter and spring, which contribute to the majority of the annual flow (*QJJA* and *QSON*). The definition of each runoff attribute and the corresponding baseline value over the study period is shown in Table 2. Note that differing from conventional hydrological studies, the nomenclature of these runoff attributes was designed to maintain consistency with the ETCCDI indices (Klein Tank et al., 2009) used for rainfall (e.g. *Pex99*), in which quantile-based indices were based on non-exceedance probabilities. Therefore, *Q99* represent the upper 1 percentile of flow, whereas *Q10* represents the lowest 10 percent of flow.

3. Methods

3.1. Overview

A schematic of the approach followed in this study is shown in Fig. 1. We first generated the climate exposure space, consisting of a large number of combinations of plausible changes in the six selected hydro-meteorological attributes related to rainfall and PET (which are visualized as three arbitrary attributes—***A***, ***B*** and ***C***—in Fig. 1). This was achieved by extending the inverse approach from Guo et al. (2016a). The approach commenced by identifying a plausible range (upper and lower limits) of change for each hydro-meteorological attribute, which was defined as being slightly wider than the uncertainty limits obtained by prior information on likely changes (e.g. from previous climate modelling studies and/or expert judgement). Synthetic hydro-meteorological time series were then simulated using a stochastic weather generator to represent different perturbation levels (Section 3.2).

Using the generated 'exposure space' (i.e. the space consisting of plausible future changes in hydro-meteorological attributes), we then conducted a climate stress test for the runoff from the case study catchment. To achieve this, GR4J was used to simulate the responses of the five runoff attributes (summarized in Table 2) to all climate perturbations obtained from the inverse approach. The runoff responses were then assessed to identify the key hydro-meteorological attributes for catchment runoff (Section 3.3), using two separate analyses:

1) The Spearman's rank coefficient correlations were first estimated between the runoff attributes and the hydro-meteorological attributes included in the climate exposure space, to detect any association between each runoff attribute and each hydro-meteorological attribute; and

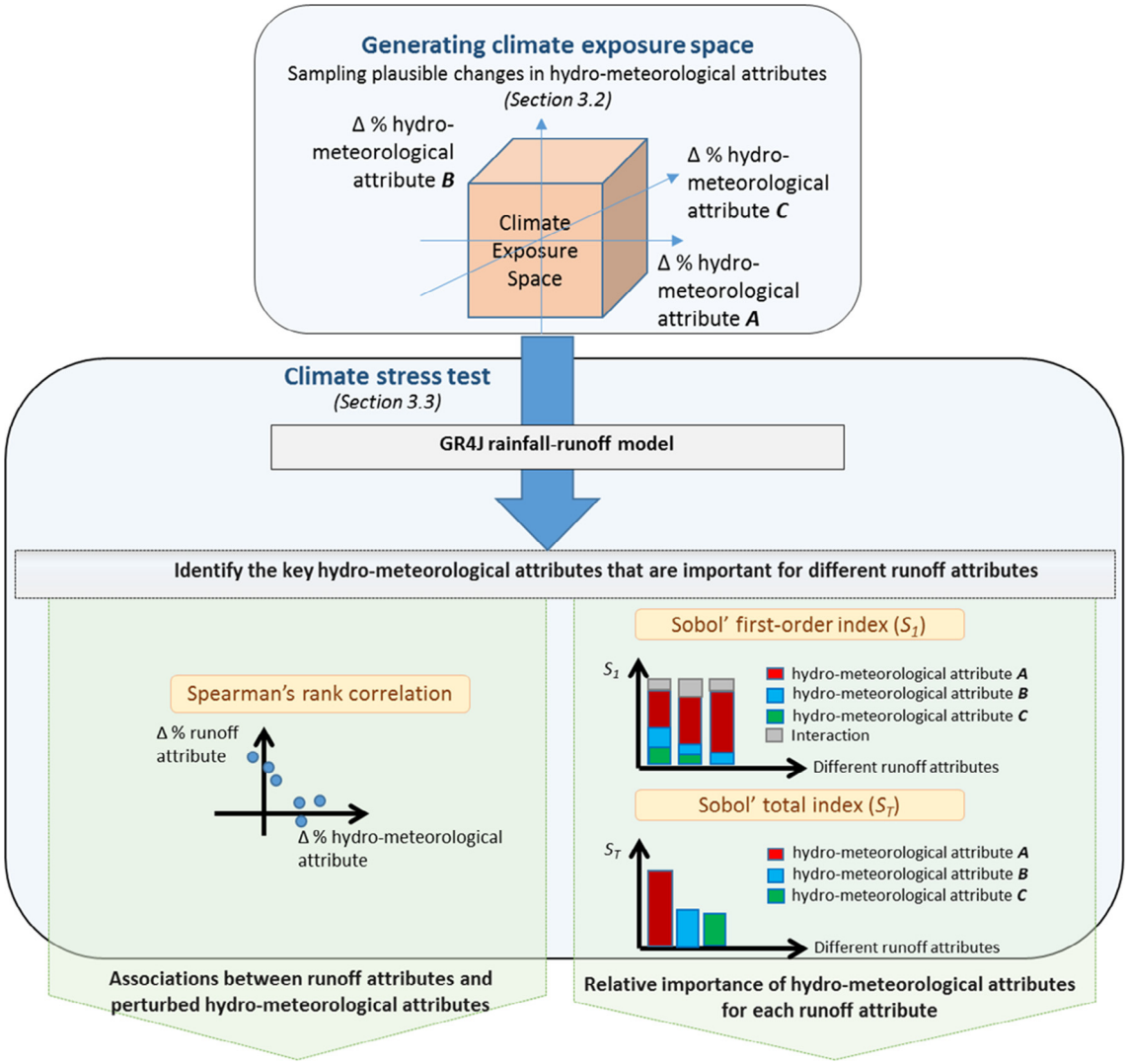

Fig. 1. Schematic of the method used in this study. Note that although the dimension of the climate exposure space was six (i.e. consisting of six hydro-meteorological attributes), it is represented in three dimensions corresponding to three arbitrary subsets *A*, *B* and *C* for ease of visualization in this figure.

2) A Sobol' sensitivity analysis (Sobol' et al., 2007, see Appendix A for details) was then used to assess the relative importance of each hydro-meteorological attribute for each runoff attribute, with the aid of the Sobol' first-order and total-order sensitivity indices. For each runoff attribute, the first-order index for each hydro-meteorological attribute represents the portion of total variance in the runoff attribute that is contributed solely by this hydro-meteorological attribute, whereas the total-order index represents the total effects of this hydro-meteorological attribute plus all its interactions with other hydro-meteorological attributes.

The specific implementation of the approach is further detailed in the sections below.

3.2. Generation of climate exposure space

The generation of the climate exposure space was undertaken in two distinct stages: (1) identification of a large number of combinations of various 'target levels' for perturbing each hydro-meteorological attribute to include in the exposure space; and (2) generation of a set of hydro-meteorological time series that corresponds to each target location within the exposure space. Each step is described in turn below.

3.2.1. Selection of the combinations of target levels in the exposure space

The first step in identifying the target values of each attribute was to specify the sampling bounds (i.e. the upper and lower limits of the exposure space), which define the ranges within which to perturb each hydro-meteorological attribute. These were determined based on recent projections of future climate conditions for the case study location by the year 2090 (CSIRO and Bureau of Meteorology, 2015; IPCC, 2014) (Table 3). The bounds were slightly wider than suggested from most climate change projections, to ensure that a comprehensive range of plausible future conditions is included in the exposure space.

Within the plausible bounds, a number of samples were drawn to define different combinations of target levels to perturb each hydro-meteorological attribute within the climate exposure space. The combinations of plausible changes in each hydro-meteorological attribute were sampled independently to ensure sufficient exploration of the entire exposure space. Latin hypercube sampling was used as the sampling method, due to its effectiveness in covering the multi-dimensional sampling spaces (Osidele

Table 3
Sampling bounds of the six hydro-meteorological attributes included in the exposure space.

Hydro-meteorological attribute	Sampling bounds
PD	−30 to +10%
Pex99	0 to +30%
PJJA	−40 to 0%
T_a	+2 to 6 °C
RH	−10 to +5%
u_z	−10 to 0%

and Beck, 2001; Sieber and Uhlenbrook, 2005; Tang et al., 2007). The numbers of samples to be included in the climate exposure space was determined according to the requirement of the Sobol' sensitivity analysis, which needs to ensure the convergence of the estimates of the Sobol' first-order and total-order sensitivity indices (as per Eqs. (A2) and (A5) in Appendix A, respectively) (Nossent et al., 2011; Zhang et al., 2015). As suggested in Zhang et al. (2015), for a particular sample size, convergence can be checked by performing 1000-fold bootstrap resampling for the estimation of the Sobol' indices, from which the mean and the 95% confidence intervals for these indices can be calculated for each input variable. Convergence is achieved if, for the input variable with the highest sensitivity, the width of 95% bootstrap confidence intervals of both of its Sobol' indices are below 10% of the corresponding means obtained from bootstrapping.

To determine the Latin hypercube sample size required by the Sobol' analysis, we generated different numbers of samples, which were then translated to the corresponding numbers of hydro-meteorological time series to simulate runoff responses as detailed in Section 3.2.2. We then estimated the Sobol' indices for these different Latin hypercube sample sizes, and tested them against the convergence conditions as specified in Zhang et al. (2015). It was observed that convergence for both Sobol' indices occurred when the sample size exceeded 2400, which was thus selected as the Latin hypercube sample size for the Sobol' sensitivity analysis. Note that for performing the Sobol' analyses for p input variables, the input samples of size n are required to be re-sampled to form a Sobol sequence with $n \times (p+2)$ elements, as detailed in Appendix A. That is, the 2400 unique Latin hypercube-derived perturbation levels in each of the six hydro-meteorological attributes were combined differently with each other, which ultimately formed a climate exposure space consisting 19200 samples.

3.2.2. Optimization-based generation of hydro-meteorological time series to achieve target levels

To generate hydro-meteorological time series corresponding to each target location in the exposure space, the stochastic weather generator WGEN (Richardson, 1981) was used. This generator has been widely applied for climate impact studies, and has generally been shown to capture most of the key features of daily rainfall series (Bastola et al., 2011; Katz, 2002; Kim et al., 2007).

WGEN uses a Markov chain model to stochastically generate daily rainfall occurrence, and a parametric distribution model to simulate rainfall intensity on wet days. The original WGEN model consists of individual monthly models for occurrence and intensity, whereas in this study, seasonal models were used to minimize the number of model parameters. For other meteorological variables such as temperature, the model divides every year into 26 intervals, and generates each meteorological variable according to its specific distributions on wet/dry days in each interval. Therefore, to generate time series related to the six hydro-meteorological attributes included in the exposure space, the following WGEN parameters were required:

- 16 parameters for rainfall, consisting of four parameters for each season: two parameters of the 1st order two-state Markov chain for representing the transition probabilities of rainfall occurrence: p_{dd} (dry–dry probability) and p_{wd} (wet–dry probability), and two parameters as the rate and shape parameters (α and β) for the Gamma distribution of rainfall intensity on wet days;
- 312 parameters for the three PET-related meteorological variables, consisting of 104 parameters to define the distribution of each variable. These include: a mean and a standard deviation during wet and dry days, respectively, for each of the 26 intervals;
- Nine parameters defining the correlation structures between the three PET-related meteorological variables, namely: six parameters for the lag-1 cross-correlations and three parameters for the lag-0 cross-correlations. Note that these correlations are for the residuals of the three meteorological variables after accounting for their individual distributions for each of the 26 intervals.

It is worth noting that WGEN was used to generate synthetic rainfall and climate time series to represent perturbed climate conditions, instead of generating replicates of historical data. Therefore, the model did not need to be calibrated to observed time series (i.e. current climate condition), but rather was calibrated through the inverse approach to achieve pre-specified target levels for each attribute. In order to generate hydro-meteorological time series corresponding to each target location, the best-fit parameter set for the WGEN model was identified using optimization. A genetic algorithm (GA) was used as the optimization engine, due to its proven efficiency, particularly for solving high-dimensional optimization problems in hydrological studies (Cheng et al., 2002; Gibbs et al., 2012; Ndiritu and Daniell, 2001; Shafii and De Smedt, 2009).

The objective function to be minimized was:

$$F_{obj,i} = \sum \sqrt{\left[\frac{(ATT^j_{s,i} - ATT_{his})}{ATT_{his}} - \frac{(\widehat{ATT}^j_{s,i} - ATT_{his})}{ATT_{his}}\right] * 100} \quad (1)$$

In Eq. (1), $j = 1, 2, \ldots 6$ for each of the six hydro-meteorological attributes considered in the exposure space (Table 1), and $i = 1, 2, \ldots n$ for n combinations of target levels in the exposure space, which corresponds to the number of samples within the exposure space (i.e. 19200, as mentioned in Section 3.2.1). For the jth hydro-meteorological attribute in the exposure space (ATT^j), $ATT^j_{s,i}$ represents the ith target value and $\widehat{ATT}^j_{s,i}$ represents the corresponding simulated value from the stochastic generator. Since different attributes are likely to have different magnitudes, the difference between a target level and the corresponding simulated level is represented as a percentage change relative to its baseline value (ATT^j_{his}) (Table 1) to ensure consistent scales across attributes during the optimization process.

When simulating the rainfall time series, since only changes in rainfall intensity were included in the exposure space (Table 1), the probability parameters (p_{dd}s and p_{wd}s) that determine the rainfall occurrences were fixed at historical levels during the optimization process. To simulate the rainfall intensity for each season, both non-negative Gamma parameters (αs and βs) were required, leading to a total of eight parameters to be determined. During the optimization process each of these parameters was varied within a range of 10^{-2} to 10. This range was identified from preliminary experiments as the optimal range for 1) quick convergence of the optimization algorithm; and 2) generation of realistic daily rainfall intensity values.

For temperature, relative humidity and wind speed, since only changes in average conditions were considered within the exposure space (Table 1), during the optimization only the mean values for wet days and dry days for each variable were varied within the corresponding plausible ranges, as defined in Table 3. To minimize the number of parameters to optimize, all other parameters, namely the standard deviation and the correlations among residuals, were fixed at corresponding historical values. Therefore, in order to generate a set of time series for these three meteorological variables, six parameters needed to be determined during the optimization process.

The optimization for each target location proceeded as follows. A wet-/dry-day sequence was first generated with the historical rainfall occurrence parameters of WGEN. Following this, four sequential optimization steps were conducted to search for the remaining WGEN parameters, aiming to fit specific target levels of different attributes. These steps consisted of:

(1) Optimizing for the best α and β parameters from the gamma distribution, which yielded the target levels of both *PD* and *Pex99* simultaneously. It is worth mentioning that the winter β used for each iteration was determined with an additional layer of optimization to achieve the target level of *PJJA*, while all other α and β values were sampled randomly;
(2) Optimizing for the best mean wet- and dry-day temperature for WGEN, to obtain the target level of T_a;
(3) Optimizing for the best mean wet- and dry-day relative humidity for WGEN, to obtain the target level of *RH*; and
(4) Optimizing for the best mean wet- and dry-day wind speed for WGEN, to obtain the target level of u_z.

The convergence criterion was set to a value of 0.1 for the objective function (Eq. (1)). In addition, as suggested in Guo et al. (2016a), during these optimization processes, the random seed of the stochastic generator was held constant. This was due to the consideration that the stochastic generator can introduce random behavior to the generated hydro-meteorological time series, which can mislead the optimization algorithm and thereby slow down the optimization process. Therefore, fixing the random seed ensured that any changes in objective function values from one iteration of the optimization process to the next were solely due to changes in the optimization decision variables (i.e. the model parameters), rather than a combination of these changes and any randomness introduced by the stochastic generator.

Following the above-mentioned optimization process, we first identified 19200 sets of best-fit WGEN parameters, corresponding to each sample point included in the climate exposure space (Section 3.2.1). We then used these parameter sets to generate 19200 sets of synthetic time series for rainfall and other hydro-meteorological variables with WGEN. The synthetic daily time series of rainfall from WGEN were used as a direct input to the calibrated GR4J model. The generated time series for the three PET-related meteorological variables (temperature, relative humidity and wind speed) were used to estimate daily PET with the Penman-Monteith model, and then fed into the calibrated GR4J model (Section 2). It is worth noting that the Penman-Monteith model requires both daily maximum and minimum time series for temperature and relative humidity as inputs. Therefore, the daily perturbations to each pair of temperature and relative humidity variables were determined by the differences between the synthetic and observed time series of daily average temperature and relative humidity. To ensure physical plausibility of the perturbations, the daily maximum and minimum values of relative humidity were capped at 100%. In addition, since solar radiation was not a meteorological attribute included in the exposure space, the historical solar radiation time series were used for estimating all sets of perturbed PET time series.

3.3. Climate stress test on catchment runoff

With the synthetic rainfall and PET time series obtained from Section 3.2, the calibrated GR4J model was run to simulate the corresponding catchment runoff. To identify the key hydro-meteorological attributes that influence catchment runoff, we first used scatter plots to visualize the association between the runoff responses and the perturbations in each hydro-meteorological attribute, with 19200 sets of synthetic hydro-meteorological time series. The Spearman's rank correlation coefficient between each runoff attribute and each hydro-meteorological attribute was also calculated to indicate the strength of the relationship between attributes. We then conducted the Sobol' analysis with the 19200 sets of hydro-meteorological time series and the corresponding runoff time series, to assess the relative importance of each hydro-meteorological attribute in influencing each runoff attribute. This analysis was implemented within the R package *sensitivity* (https://cran.r-project.org/web/packages/sensitivity/index.html). Both the Sobol' first- and total-order sensitivity indices for each runoff attribute were estimated (as Eqs. (A2) and (A5) in Appendix A, respectively), which indicate how much the total variance of the runoff was due to the individual contribution of each individual hydro-meteorological attribute and how much of this was due to the interactions among multiple attributes.

4. Results

4.1. Performance of inverse approach

The performance of the inverse approach in terms of its ability to generate the desired climate exposure space (Section 3.2) is shown in Fig. 2, as pairs plots of the sampled changes relative to the baseline level for each of the six hydro-meteorological attributes (as specified in Table 1). We illustrate this with the 2400 samples obtained from Latin hypercube sampling, as it consists of fewer samples than the full sample set included in the exposure space (19200 samples), and therefore allows for clearer visualization. As can be seen, the inverse approach is effective in producing the desired target sampling locations, with all samples falling within the bounds of the exposure space (as defined in Table 3). In addition, the coverage of the climate exposure space is relatively uniform, with low correlations (i.e. independence) between each pair of hydro-meteorological attributes. Therefore, the exposure spaces generated with the inverse approach enable us to assess the sensitivity of catchment runoff to a wide range of plausible climate conditions.

4.2. Key hydro-meteorological attributes for catchment runoff

4.2.1. Spearman's rank correlation coefficients

The responses of the five runoff attributes to the 19200 sets of perturbed hydro-meteorological attributes within the exposure space are plotted in Fig. 3, as percentage changes relative to the corresponding baseline levels. The correlation between each runoff attribute and each hydro-meteorological attribute is summarized in Table 4 in terms of Spearman's rank correlation coefficients (ρ), with bolded figures indicating correlations that are significant at a 0.05 level ($p < 0.05$). Overall, the runoff attributes show strongest correlations with *PJJA*, followed by the *PD*. Also, common to all runoff attributes is that the three hydro-meteorological attributes related to PET (T_a, *RH* and u_z) generally have very low correlations

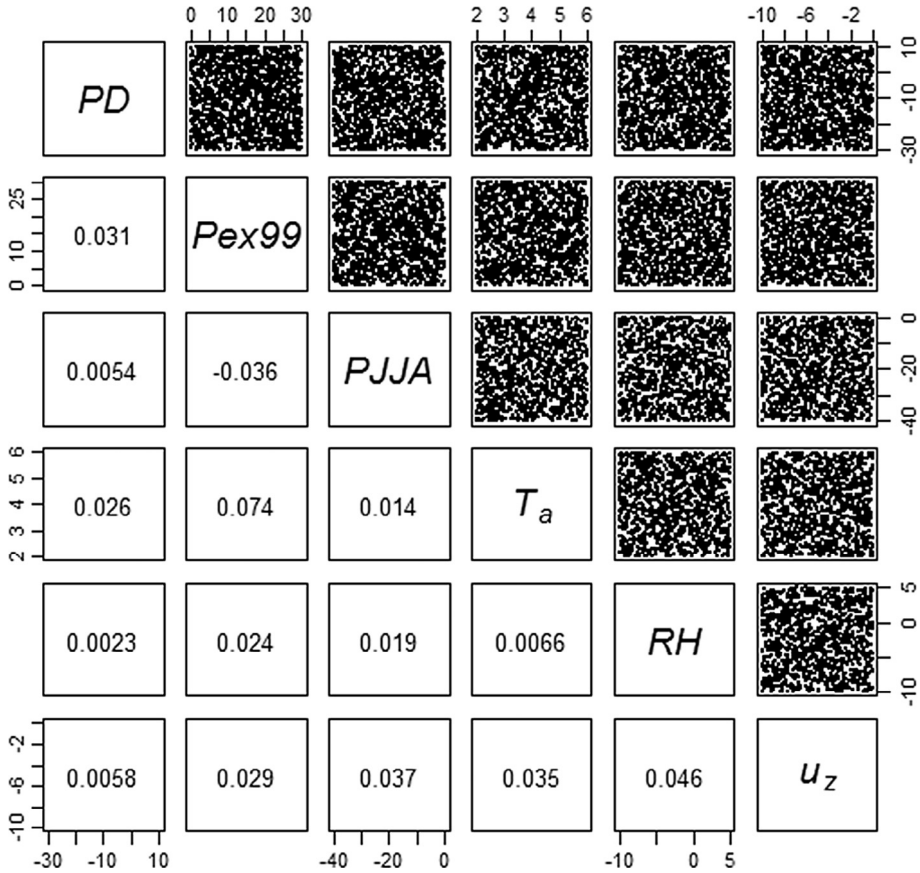

Fig. 2. Climate exposure space consisting of 2400 Latin hypercube samples generated with the inverse approach, described as a percentage change for *PD*, *Pex99*, *PJJA*, *RH* and u_z, and absolute changes for T_a (in °C), relative to the corresponding baseline levels (Table 1). The lower-left triangle displays pairwise Spearman's correlation coefficients.

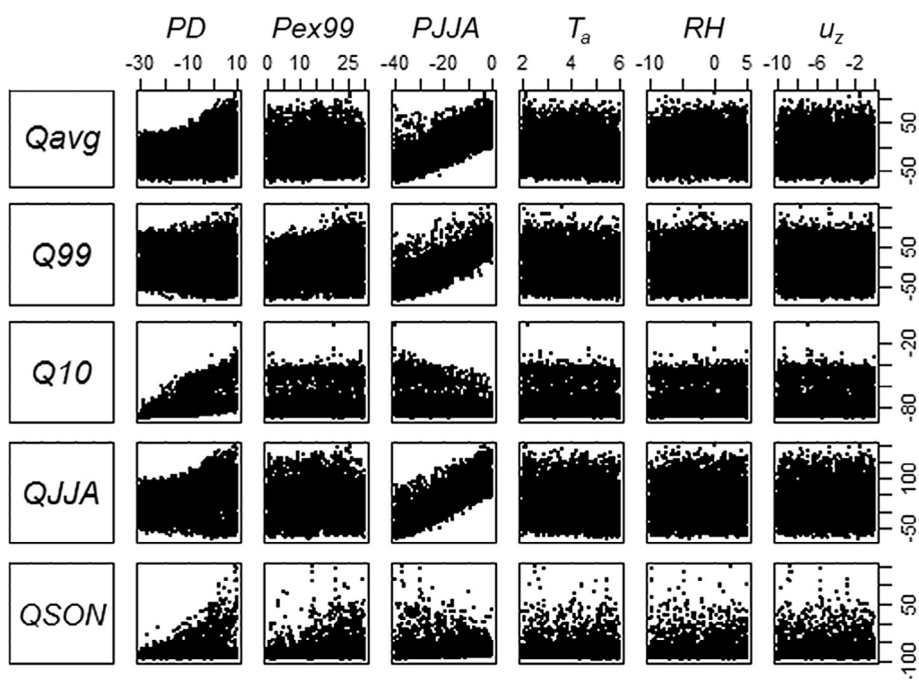

Fig. 3. Responses of the five runoff attributes (as percentage changes relative to the baseline levels) to 19200 perturbations of the six hydro-meteorological attributes considered in the exposure space.

Table 4
Spearman's rank correlation coefficients (ρ) between the five runoff attributes and the six hydro-meteorological attributes considered in the exposure space, as plotted in Fig. 3. Bolded figures indicate that correlations are significant at the 0.05 level.

	PD	*Pex99*	*PJJA*	T_a	*RH*	u_z
Qavg	**0.305**	0.008	**0.725**	**−0.073**	**0.051**	0.002
Q99	**−0.039**	**0.175**	**0.836**	**−0.055**	**0.038**	0.01
Q10	**0.783**	**−0.103**	**−0.398**	**−0.054**	**0.051**	−0.011
QJJA	**0.153**	−0.01	**0.789**	**−0.059**	**0.036**	0.007
QSON	**0.158**	**0.12**	**0.453**	**−0.128**	**0.094**	**−0.017**

with the runoff attributes, with the absolute magnitudes of most ρ less than 0.1.

Table 4 shows that the Spearman correlation coefficients vary across different runoff attributes. However, a common pattern is observed within the runoff attributes that are related to high flows, as they all display strong associations with winter rainfall. Specifically, *Qavg*, *Q99* and *QJJA* all show high correlations with *PJJA* (with ρ values of 0.725, 0.836 and 0.789, respectively, which are all significant at the 0.05 level), with strong near-linear relationships illustrated in Fig. 3. Following *PJJA*, the second most influencing hydro-meteorological attribute is *PD* for *Qavg* and *QJJA* (with correlation coefficients of 0.305 and 0.153, respectively, significant at the 0.05 level), whereas *Q99* shows a significant correlation with *Pex99* ($\rho = 0.175$). This indicates that it is the seasonality of the rainfall, rather than the total annual rainfall *per se*, that appears to be the strongest driver for most of the runoff attributes considered. This applies equally for extreme runoff (*Q99*), which is shown to be much more sensitive to winter rainfall than to extreme rainfall of the same quantile (i.e. *Pex99*).

In contrast to the above finding, as an indicator of low flow, *Q10* illustrates a somewhat opposite pattern to those shown for *Qavg*, *Q99* and *QJJA*, as it displays the highest correlation with *PD* ($\rho = 0.783$), followed by a moderate negative correlation with *PJJA* ($\rho = -0.398$). Another contrasting response is observed in *QSON*, which does not show a particularly high correlation with any rainfall attribute. The strongest correlation is with *PJJA*, with a correlation coefficient of only 0.453. In addition, ET shows a greater impact on *QSON* compared with other runoff attributes, with T_a showing a ρ value of −0.128. The higher sensitivity of runoff to temperature during spring can be a combined result of fuller catchment storage and rising temperature in this season.

It is worth noting that *Q10* shows negative correlations with *PJJA* and *Pex99*, which is likely to be explained by the method of climate perturbation: as multiple rainfall attributes have been perturbed at the same time during the inverse approach, for a specific average rainfall intensity (*PD*), an increase in winter/extreme rainfall (*PJJA*/*Pex99*) has to be achieved by reducing the low rainfall intensity and/or rainfall during the drier seasons, which is likely to lead to a decrease in low flow (*Q10*).

4.2.2. Sobol' sensitivity analysis

Having assessed the correlations between the five runoff attributes and the six hydro-meteorological attributes included in the exposure space, we now quantify the relative importance of each attribute for the runoff attributes by using the Sobol' indices. The Sobol' first-order indices of each hydro-meteorological attribute, as well as their interactions, are presented in Fig. 4, and are plotted against the five different runoff attributes. For each runoff attribute, the sum of the first-order indices for all hydro-meteorological attributes, and the total effect of their interactions, equals one (as in Eq. (A6) in Appendix A).

Consistent with the correlation results in Section 4.2.1, the first-order indices generally suggest that the two most important hydro-meteorological attributes for runoff are *PJJA*, followed by *PD*. Again, the runoff attributes that are related to high flows show similar sensitivity patterns. Specifically, for *Qavg*, *Q99* and *QJJA* the first-order indices of *PJJA* always exceed 0.5 (0.513, 0.757 and 0.634, respectively), indicating that more than half of the variation in the responses of each of these runoff attributes is contributed by perturbations in *PJJA*. Following *PJJA*, *PD* is the second most important variable for *Qavg* and *QJJA* (with index values of 0.161 and 0.086, respectively), while *Pex99* is the second most important variable for *Q99* (with an index value of 0.052).

In contrast to *Qavg*, *Q99* and *QJJA*, the first-order indices for *Q10* suggest that *PD* is the dominant variable (with an index value of 0.548), whereas for *QSON*, the importance of *PD*, *Pex99* and *PJJA*

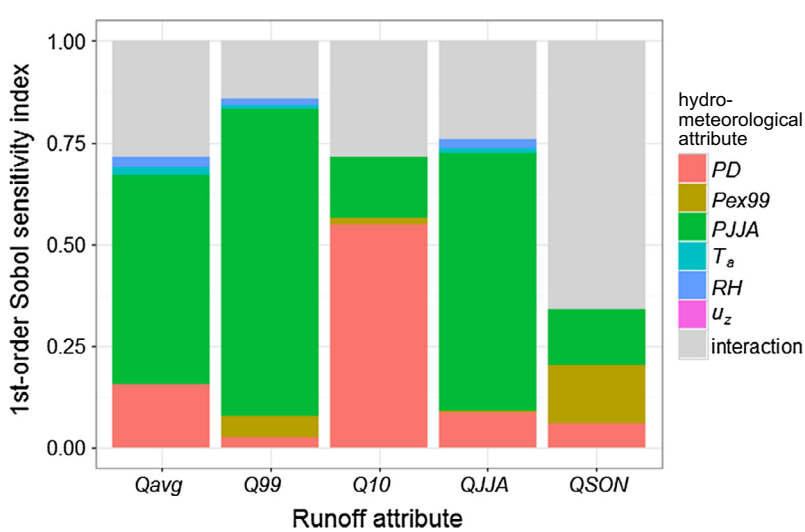

Fig. 4. Sobol' first-order sensitivity of the five runoff attributes to changes in the six hydro-meteorological attributes (colored) and their interaction effects (grey). (For interpretation of the references to colour in this figure legend, the reader is referred to the web version of this article.)

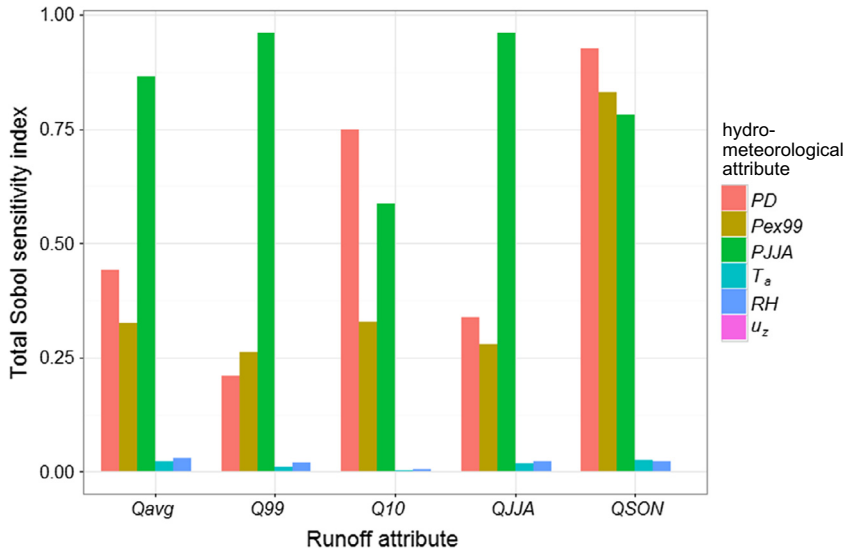

Fig. 5. Sobol' total-order sensitivity of the five runoff attributes to changes in the six hydro-meteorological attributes.

are of similar magnitude (with index values of 0.058, 0.143 and 0.146, respectively). Lastly, T_a, *RH* and u_z all show first-order indices below 0.03 for all runoff attributes, which again indicates low impact of PET-related changes on runoff.

In addition to providing confirmation of the results obtained using the correlation analysis (Section 4.2.1), the Sobol' analysis also provides information on the interactions among the six hydro-meteorological attributes (grey bars in Fig. 4). As can be seen, the two runoff attributes that are least affected by these interactions are *Q99* and *QJJA*, with both interaction terms having values below 0.25. In contrast, the interactions are slightly higher for *Qavg* (0.285) and *Q10* (0.284), and significantly higher for *QSON* (0.660), with more than 60% of the total variance contributed by interactions, rather than changes in individual hydro-meteorological attributes.

The interaction effects are also reflected in Fig. 5, which shows the Sobol' total-order sensitivity indices of the six hydro-meteorological attributes for each runoff attribute. For each runoff attribute, the total-order index of each hydro-meteorological attribute represents the sum of its individual effect and all its interaction with other hydro-meteorological attributes (as in Eq. (A5), Appendix A). For example, the total-order index of *Qavg* to *PD* indicates not only the individual effect that *PD* has on *Qavg*, but also the effects of all interactions among *PD* and the other five hydro-meteorological attributes. Therefore, comparing the total order index with the first-order index (in Fig. 4) can help us to assess the magnitude of the interaction effects from each hydro-meteorological variable in influencing runoff. By comparing Figs. 5 to 4, it is clear that the most distinct differences between the total order and the first-order indices are for *QSON*, with much higher total-order indices to *PD*, *Pex99* and *PJJA* (0.749, 0.328 and 0.588, respectively) compared to their corresponding first-order indices (as 0.058, 0.143 and 0.146, respectively). Consistent with Fig. 4, this highlights the importance of the interactions among the three hydro-meteorological attributes for *QSON*, in which the relative importance of the interaction effects exceed that of any individual attribute.

5. Discussion

5.1. Linking the results with catchment characteristics

This study sought to expand the scope of scenario-neutral studies to consider possible changes in a broader range of hydro-meteorological attributes, to account for not only mean changes in key atmospheric drivers but also the extremes and seasonality. The results from the correlation and Sobol' sensitivity analyses presented in Section 4 highlight the relative importance of the various hydro-meteorological attributes considered for simulated runoff generation for the Scott Creek catchment, which clearly reflect the unique catchment characteristics. As illustrated in both analyses, winter rainfall (*PJJA*) was found to be a key hydro-meteorological attribute for this catchment, and has a substantial impact on the average and extreme runoff (*Qavg* and *Q99*) as well as the winter runoff (*QJJA*). The high sensitivity of average runoff to changes in winter rainfall clearly illustrates the winter-dominated nature for both rainfall and runoff in the Scott Creek catchment, which is consistent with previous literature (Westra et al., 2014a, b). This high sensitivity in winter also indicates the importance of high antecedent soil moisture for a small-sized catchment, which influences the conversion from rainfall to runoff such that a unit of rain falling in winter leads to much greater runoff than a unit of rain falling in summer. Interestingly, the extreme runoff was found to be much more sensitive to the winter rainfall than to the extreme rainfall (*Pex99*), highlighting that accumulations of continuous rainfall events over winter are likely to have higher impacts on runoff compared to individual extreme rainfall events. In contrast to the abovementioned, runoff attributes that are related to the high flows, the low flow (*Q10*) is dominantly driven by average rainfall (*PD*), which reflects the heavy-tailed nature of the distribution of daily runoff.

The results also suggest that potential changes in PET generally have a low impact on runoff from the Scott Creek catchment. This is likely to be related to the water-limited nature of the catchment, for which the long-term average rainfall is substantially lower than the long-term average PET (McVicar et al., 2010). From a water-balance perspective, since PET represents the upper limit of actual ET (AET), the AET from such a water-limited catchment is likely to be lower than PET for the majority of the year, which leads to low sensitivity of AET to any changes in PET. Among the three PET-related hydro-meteorological variables, T_a shows the highest impact on runoff, which is consistent with a previous finding, which showed that temperature is the most important driver affecting PET in the case study catchment (Guo et al., 2017).

Although some of the dominant features of runoff response are well known (e.g. the catchment sensitivity to winter rainfall), others are somewhat more surprising, such as the importance of winter rainfall rather than extreme rainfall in driving extreme flow

(defined as the 99th percentile daily rainfall and flow, respectively). The consistency of the study results with this *a priori* understanding provides a way of verifying the modelled runoff sensitivity and correlation with its driving hydro-meteorological attributes. Furthermore, the study results also illustrate potential new insights into the hydrological controls on catchment response, which highlights the value of applying scenario-neutral analysis as a means of improving the current understanding of catchment characteristics, as well as identifying the key attributes that would be expected to affect hydrological response under a changing climate, for any particular catchment.

The above results also highlight the importance of considering various attributes for each hydro-meteorological variable, such as sub-annual features and extremes, in the design of climate exposure spaces for scenario-neutral approaches. For example, the seasonal results are particularly pertinent for Scott Creek catchment, as projections for climate change suggest potentially much stronger seasonal changes compared to annual average changes, with higher projected declines for rainfall during the wet (i.e. winter) months compared to all other seasons (CSIRO and Bureau of Meteorology, 2015; IPCC, 2014). Therefore, this study has made an important advance to previous implementations of scenario-neutral approach, by starting to incorporate seasonal changes in hydro-meteorological attributes in a realistic manner (i.e. via a weather generator). However, despite the insights obtained from analyzing six hydro-meteorological variables in this scenario-neutral analysis, the full range of potential changes are likely to be much greater (e.g. including other types of seasonal changes, modifications in rainfall intermittency and number of wet days, and so on) and these have not been explored in the current study. This is a key limitation which will be further discussed in the subsequent section.

5.2. Limitations and future works

As one of the initial implementations to explore a more complex exposure space in scenario-neutral approaches, this study focuses on illustrating the capacity of the improved scenario-neutral approach with a simplified study design. It is therefore important to acknowledge the limitations that are likely to affect the results. We first illustrate how the limitation of considering only six hydro-meteorological attributes in the exposure space can affect the study results. As can be seen in Fig. 4, spring runoff (*QSON*) shows substantial sensitivity to interactions among the hydro-meteorological attributes, which exceeds that for any individual attribute. An obvious interpretation of these results is that spring runoff is driven by more complex processes that involve non-linear interactions of the hydro-meteorological attributes, under the assumption that all key hydro-meteorological attributes that influence spring runoff have been included in the climate exposure space. However, an alternative explanation is provided in Fig. 6, which is an expanded version of Fig. 3, in which the corresponding *PSON* obtained from each of the 19200 generated rainfall time series used in the correlation analyses is also shown. It is clear that *QSON* shows a strong correlation with *PSON*. This indicates that the changes in *QSON* are likely to be predominantly driven by *PSON*, which changes as a result of perturbing other hydro-meteorological attributes with the stochastic generator. However, since *PSON* was not considered in our design of the climate exposure space and was not sampled together with the other hydro-meteorological attributes, these impacts from varying *PSON* were not recognized by the Sobol' analysis. Since all first-order indices and interaction effects sum up to one for *QSON*, the possible 'missing' individual effect of *PSON* leads to an increase in the portion of interaction effects identified for *QSON* from the Sobol' analysis, as illustrated in Fig. 4.

The potential impact of omitting the spring rainfall illustrates that the exclusion of relevant hydro-meteorological attributes in the exposure space can lead to misinterpretation of the sensitivity results obtained from scenario-neutral approaches. Therefore, it is expected that for designing a more comprehensive scenario-neutral assessment of potential climate impacts, the climate exposure space should be expanded by considering a greater number of rainfall and other hydro-meteorological attributes. This is particularly important for catchments with highly seasonal variations in rainfall and streamflow regimes, as they are likely to be driven by different hydrological processes during different seasons and thus respond differently to changes in hydro-meteorological conditions across seasons (e.g. Barnett et al., 2005; Chang and Jung, 2010; Sorg et al., 2012). Besides, statistics related to variance, persistence and extremes are likely linked with the occurrence of extreme events such as floods and droughts (Bewket and

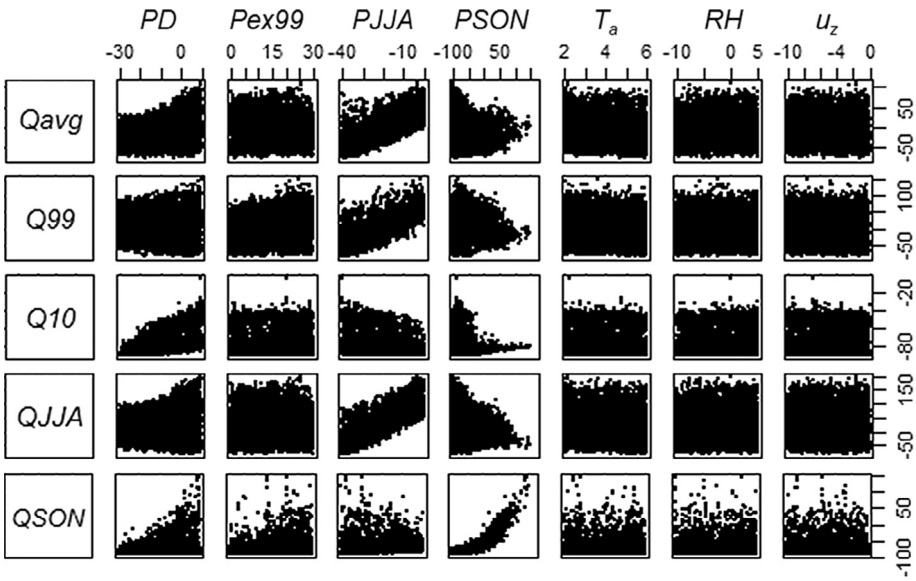

Fig. 6. Responses of the five runoff attributes (as percentage changes relative to the historical levels) to 19200 perturbations of the six hydro-meteorological attributes considered in the exposure space, as well as to *PSON*, which was modified as a result of perturbing the six attributes.

Conway, 2007; Müller et al., 2009) and should thus also be considered.

With all these considerations, a persisting question for future implementations of the scenario-neutral approach will be whether a sufficient number of hydro-meteorological attributes has been considered. As a starting point, it is reasonable to utilize any prior knowledge of important hydro-climate processes for the case study, as well as future projections that might suggest critical changes in some hydro-meteorological attributes. To improve the comprehensiveness of the approach, there is a potential need of some iterative approach, as illustrated in the abovementioned example with spring rainfall. Nevertheless, the scenario-neutral framework is showing the capability to incorporate a large number of hydro-climatic attributes, which is critical to drive a comprehensive climate impact assessment for particular case studies.

In some cases, the structure of the stochastic weather generator can provide a limitation on the number of attributes that can be modified as part of developing an exposure space. This can be potentially improved by considering more advanced techniques to generate synthetic climate time series. These include alternative choices of stochastic weather generators that are more complex and flexible than the WGEN illustrated in this study. An example of such a weather generator is the UK Climate Projections (UKCP09) weather generator, which uses a Neymann-Scott Rectangular Processes (NSRP) rainfall generator, for its good performance in modelling the clustered nature of rainfall occurrence; once the rainfall time series is generated, other hydro-meteorological time series can be generated with distribution models depending on the wet/dry status of not only the current but also the preceding day (Jones et al., 2011; Kilsby et al., 2007). Other parametric models for statistical downscaling that can also be employed within this framework, such as the Decision Centric version of the Statistical DownScaling Model (SDSM-DC), which enables manipulation of various statistics of the observed rainfall and climate time series, including wet/dry day occurrence, mean, variance and temporal trend (Wilby et al., 2014). The parametric nature of these methods means that they can also be optimized as illustrated for WGEN in this study, and thus can be easily incorporated into the scenario-neutral framework. It is expected that these more flexible climate perturbation models can greatly expand the capacity of scenario-neutral approaches, so that a larger number of hydro-meteorological attributes can be considered with higher levels of constraints imposed within each climate time series (e.g. perturbing seasonal and monthly attributes and extremes within the same time series).

It is worth noting that the above-mentioned improvements in climate perturbation can be associated with substantial increases in the difficulty as well as computational effort for the optimization processes used in implementing the scenario-neutral approach. This can be firstly caused by the use of more flexible models for climate perturbation, which generally include a larger number of parameters (Jones et al., 2011; Kilsby et al., 2007; Semenov, 2007; Wilby et al., 2014), resulting in larger search spaces for the optimization process and therefore making it more difficult to determine the parameter sets used for constructing the climate exposure space. Furthermore, the optimization process is also more difficult and computationally expensive as the consideration of more hydro-meteorological attributes also requires the inclusion of more constraints on the time series for each hydro-meteorological variable. For example, in this study, we have considered a number of plausible changes in three rainfall attributes as statistics from a single rainfall time series (i.e. the average and 99th percentile of rainfall intensity, and winter average values). This was achieved by the implementing the staged optimization processes outlined in Section 3.2.2. However, once the number of hydro-meteorological attributes to consider increases, more systematic approaches should be designed to maintain reasonable efficiency of optimization. These challenges warrant future studies on seeking to balance the capability of climate perturbation and computational effort.

Since the study results represent sensitivity of simulated runoff, an additional issue relates to the extent to which hydrological modelling is able to simulate catchment response under perturbed climates. This issue was raised in several previous papers (Coron et al., 2012; Kirchner, 2006; Wagener et al., 2003; Westra et al., 2014a), which highlight that catchment models calibrated to one climate regime (e.g. the historical climate) may not perform as well under changed climate regimes, due to issues related to model realism and parameter non-stationarity. Therefore, although GR4J has shown reasonable performance against the historical climate in Scott Creek (Guo et al., 2017; Westra et al., 2014a,b), the model may under- or over-estimate hydrological sensitivity to modified climate regimes, as this aspect of model performance has undergone limited evaluation under a changing climate. Therefore, a comprehensive application of the scenario-neutral approach should consider simulations from a number of structurally different rainfall-runoff models, which include models with alternative lumped structures (e.g. Oudin et al., 2005), as well as physically-based models with more explicit representation of specific hydrological processes (e.g. base flow and inter-flow), and/or detailed consideration of catchment heterogeneity (e.g. land cover types, grid cells and vertical layers) (Clark et al., 2011; Harrigan et al., 2014). Furthermore, the plausibility of these modelled results can be further verified with historical observations over time periods of sufficient length, via model-independent method such as elasticity analysis (Fu et al., 2011; Prudhomme et al., 2015). Although considering these alternative conceptualizations and representations of physical processes cannot guarantee that the models successfully represent all possible changes in catchment runoff, using an ensemble of modelling approaches can greatly enhance our understanding of the plausible range of runoff responses to potential climate change conditions.

6. Conclusions

In this study, we illustrated a formal implementation of the scenario-neutral approach, in order to identify the key climatic attributes influencing different runoff attributes from the Scott Creek catchment in South Australia. To achieve this, we first extended the applicability of a recently developed inverse approach to enable stochastic generation of a climate exposure space, which enables generation of synthetic time series to represent plausible future changes in a large number of hydro-meteorological variables and their attributes. Specifically, we generated time-series for: (1) rainfall, to represent plausible future changes in its average conditions, extremes and seasonal patterns; and (2) three meteorological variables related to PET (i.e., temperature, relative humidity, and wind speed), to represent plausible changes in their mean values. With these synthetic hydro-meteorological time series, we simulated potential changes in catchment runoff with a conceptual rainfall-runoff model, GR4J. By investigating the relationships between runoff responses and perturbations in each hydro-meteorological attribute using both correlation and Sobol' sensitivity analyses, we identified the key hydro-meteorological attributes that can greatly influence different runoff attributes from the catchment considered.

The results from this study show that different runoff attributes are dominated by changes in the rainfall attributes, while the PET-related variables have a relatively minor effect. Specifically:

- The runoff attributes that are related to high-flow, namely average runoff, extreme runoff and winter runoff, show substantial sensitivity to winter rainfall, followed by average rainfall;

- The runoff attribute that is related to low-flow is mainly affected by changes in average rainfall; and
- Spring runoff displays higher sensitivity to the interactions among the rainfall attributes, compared with any individual contributions, possibly as a result of the insufficient number of hydro-meteorological attributes considered in the case study.

The key hydro-meteorological attributes highlighted for different runoff attributes are closely linked to the unique characteristics of the case study catchment, which exhibits significant seasonal variations in not only the rainfall and runoff, but also the key processes involved in converting rainfall to runoff. These results also highlight the need to design individual implementations of scenario-neutral approaches for specific case studies, as different water resource systems are likely to be driven by different hydro-meteorological attributes and key processes (e.g. Gaál et al., 2012; Merz and Blöschl, 2009; van der Kamp et al., 2003), which can lead to identification of different sets of key hydro-meteorological attributes for each individual system. The unique features of individual catchments mean that findings for the Scott Creek catchment are difficult to translate to other catchments, potentially even those with relatively similar hydro-climatic regimes (e.g. Beven, 2000). Nevertheless, this study provides a 'proof-of-concept' that highlights the capacity of the scenario-neutral approach to enhance our understanding of water resource systems. Furthermore, as one of the initial implementations of the scenario-neutral approaches to a more complex exposure space, this study identified several critical improvements to be made in future implementations, with the ultimate goal being to extend the scenario-neutral concept to a comprehensive range of possible future climates.

Acknowledgements

The authors wish to thank the two anonymous reviewers for their thoughtful comments on the manuscript.

Appendix A.

Sobol' sensitivity analysis (Sobol' et al., 2007)

Sobol' is considered a variance-based method, in which the total variance in a model output due to changes in its inputs is estimated with a Monte-Carlo approach. To estimate the variances, a large number of samples is firstly drawn by varying all input variables at the same time, and then a Sobol sequence is constructed by re-sampling from within these Monte-Carlo samples (Saltelli et al., 2010). According to Sobol' et al. (2007), to estimate the Sobol' first-order and total-order indices with a Monte-Carlo sample size of n consisting of p input variables, a Sobol sequence with a total of $n \times (p+2)$ samples is required, i.e. with $n \times (p+2)$ model evaluations.

The total variance of model output is partitioned to the contribution of each individual input variable (i.e. first-order effects), as well as their interactions (i.e. higher-order effects), as follows (equation adapted from Zhang et al., 2015):

$$V_Y = \underbrace{\sum_{i=1}^{p} V_i}_{\text{Individual effects}} + \underbrace{\sum_{i<j}\sum_{i<j} V_{ij} + \sum_{i<j<k} V_{ijk} \ldots + V_{1,2\ldots,p}}_{\text{Interactions}} \tag{A1}$$

The outputs from the Sobol' method comprise (equations adapted from Nossent et al., 2011):

1) First-order sensitivity index, which quantifies the individual contribution of each input variable to the total variance of the model's output:

$$S_i = \frac{V_i}{V_Y} \tag{A2}$$

2) Second- and higher-order sensitivity indices, which quantify the contribution of interactions among two or more input variables to the total variance of the model's output:

$$\text{For second} - \text{order}: S_{ij} = \frac{V_{ij}}{V_Y} \tag{A3}$$

$$\text{For higher} - \text{order}: S_{ij\ldots n} = \frac{V_{ij\ldots p}}{V_Y} \tag{A4}$$

3) Total sensitivity index, which quantifies the contribution of each input variable, including its individual effect, as well as all its interactions with other input variables, to the total variance of the model's output:

$$S_{Ti} = S_i + \sum_{j \neq i} S_{ij} = 1 - \frac{V_{\sim i}}{V_Y} \tag{A5}$$

From Eqs. (A1)(A4), the sum of individual effects of all input variables and all their interactions equals one (adapted from Zhang et al., 2015):

$$1 = \underbrace{\sum_{i=1}^{p} S_i}_{\text{Individual effects}} + \underbrace{\sum_{i<j}\sum_{i<j} S_{ij} + \sum_{i<j<k} S_{ijk} \ldots + S_{1,2\ldots,p}}_{\text{Interactions}} \tag{A6}$$

References

Allen, R.G., Pereira, L.S., Raes, D., Smith, M., 1998. Crop evapotranspiration-Guidelines for computing crop water requirements-FAO irrigation and drainage paper 56. FAO, Rome 300 (9), D05109.

Barnett, T.P., Adam, J.C., Lettenmaier, D.P., 2005. Potential impacts of a warming climate on water availability in snow-dominated regions. Nature 438 (7066), 303–309.

Bastola, S., Murphy, C., Sweeney, J., 2011. The sensitivity of fluvial flood risk in Irish catchments to the range of IPCC AR4 climate change scenarios. Sci. Total Environ. 409 (24), 5403–5415. http://dx.doi.org/10.1016/j.scitotenv.2011.08.042.

Beven, K.J., 2000. Uniqueness of place and process representations in hydrological modelling. Hydrology and Earth System Sciences (HESS) & Discussions (HESSD).

Bewket, W., Conway, D., 2007. A note on the temporal and spatial variability of rainfall in the drought-prone Amhara region of Ethiopia. Int. J. Climatol. 27 (11), 1467–1477. http://dx.doi.org/10.1002/joc.1481.

Brown, C., Ghile, Y., Laverty, M., Li, K., 2012. Decision scaling: linking bottom-up vulnerability analysis with climate projections in the water sector. Water Resour. Res. 48 (9), W09537. http://dx.doi.org/10.1029/2011WR011212.

Brown, C., Werick, W., Leger, W., Fay, D., 2011. A decision-analytic approach to managing climate risks: application to the Upper Great Lakes1. JAWRA J. Am. Water Resour. Assoc. 47 (3), 524–534. http://dx.doi.org/10.1111/j.1752-1688.2011.00552.x.

Brown, C., Wilby, R.L., 2012. An alternate approach to assessing climate risks. Eos Trans. Am. Geophys. Union 93 (41), 401–402.

Chang, H., Jung, I.-W., 2010. Spatial and temporal changes in runoff caused by climate change in a complex large river basin in Oregon. J. Hydrol. 388 (3–4), 186–207. http://dx.doi.org/10.1016/j.jhydrol.2010.04.040.

Cheng, C.T., Ou, C.P., Chau, K.W., 2002. Combining a fuzzy optimal model with a genetic algorithm to solve multi-objective rainfall–runoff model calibration. J. Hydrol. 268 (1–4), 72–86. http://dx.doi.org/10.1016/S0022-1694(02)00122-1.

Chiew, F.H.S., McMahon, T.A., 1991. The applicability of Morton's and Penman's evapotranspiration estimates in rainfall-runoff modelling. JAWRA J. Am. Water Resour. Assoc. 27 (4), 611–620.

Clark, M.P., Kavetski, D., Fenicia, F., 2011. Pursuing the method of multiple working hypotheses for hydrological modeling. Water Resour. Res. 47 (9), W09301. http://dx.doi.org/10.1029/2010WR009827.

Coron, L., Andréassian, V., Perrin, C., Lerat, J., Vaze, J., Bourqui, M., Hendrickx, F., 2012. Crash testing hydrological models in contrasted climate conditions: An experiment on 216 Australian catchments. Water Resources Research 48 (5). http://dx.doi.org/10.1029/2011WR011721.

CSIRO and Bureau of Meteorology, 2015. Climate Change in Australia Information for Australia's Natural Resource Management Regions: Technical Report. CSIRO and Bureau of Meteorology, Australia.
Culley, S., Noble, S., Yates, A., Timbs, M., Westra, S., Maier, H.R., Giuliani, M., Castelletti, A., 2016. A bottom-up approach to identifying the maximum operational adaptive capacity of water resource systems to a changing climate. Water Resour. Res. 52 (9), 6751–6768. http://dx.doi.org/10.1002/2015WR018253.
Dessai, S., Hulme, M., 2004. Does climate adaptation policy need probabilities? Clim. Policy 4 (2), 107–128.
Evans, J.P., Jakeman, A.J., 1998. Development of a simple, catchment-scale, rainfall-evapotranspiration-runoff model. Environ. Modell. Software 13 (3–4), 385–393. http://dx.doi.org/10.1016/S1364-8152(98)00043-7.
G. Fu, F. Chiew, S. Charles, F. Mpelasoka, Assessing precipitation elasticity of streamflow based on the strength of the precipitation-streamflow relationship, in: Proceedings of the 19th International Congress on Modelling and Simulation, 2011, pp. 3567–3572.
Gaál, L., Szolgay, J., Kohnová, S., Parajka, J., Merz, R., Viglione, A., Blöschl, G., 2012. Flood timescales: understanding the interplay of climate and catchment processes through comparative hydrology. Water Resour. Res. 48 (4). http://dx.doi.org/10.1029/2011WR011509.
Gibbs, M.S., Maier, H.R., Dandy, G.C., 2012. A generic framework for regression regionalization in ungauged catchments. Environ. Modell. Software 27–28, 1–14. http://dx.doi.org/10.1016/j.envsoft.2011.10.006.
Guo, D., Westra, S., Maier, H.R., 2016a. An inverse approach to perturb historical rainfall data for scenario-neutral climate impact studies. J. Hydrol. http://dx.doi.org/10.1016/j.jhydrol.2016.03.025.
Guo, D., Westra, S., Maier, H.R., 2016b. An R package for modelling actual, potential and reference evapotranspiration. Environ. Modell. Software 78, 216–224. http://dx.doi.org/10.1016/j.envsoft.2015.12.019.
Guo, D., Westra, S., Maier, H.R., 2016c. Sensitivity of potential evapotranspiration to changes in climate variables for different climatic zones. Hydrol. Earth Syst. Sci. Discuss. 2016, 1–43. http://dx.doi.org/10.5194/hess-2016-441.
Guo, D., Westra, S., Maier, H.R., 2017. Impact of evapotranspiration process representation on runoff projections from conceptual rainfall-runoff models. Water Resour. Res. 53. http://dx.doi.org/10.1002/2016WR019627.
Harrigan, S., Murphy, C., Hall, J., Wilby, R.L., Sweeney, J., 2014. Attribution of detected changes in streamflow using multiple working hypotheses. Hydrol. Earth Syst. Sci. 18 (5), 1935–1952. http://dx.doi.org/10.5194/hess-18-1935-2014.
IPCC, Climate Change 2014: Impacts, Adaptation, and Vulnerability. Part A: Global and Sectoral Aspects, in: Contribution of Working Group II to the Fifth Assessment Report of the Intergovernmental Panel on Climate Change, Cambridge, United Kingdom and New York, NY, USA, 2014.
Jones, P., Harpham, C., Goodess, C., Kilsby, C., 2011. Perturbing a weather generator using change factors derived from regional climate model simulations. Nonlinear Processes Geophys. 18 (4), 503–511.
Katz, R.W., 2002. Techniques for estimating uncertainty in climate change scenarios and impact studies. Clim. Res. 20 (2), 167–185.
Kay, A.L., Crooks, S.M., Reynard, N.S., 2014. Using response surfaces to estimate impacts of climate change on flood peaks: assessment of uncertainty. Hydrol. Processes 28 (20), 5273–5287. http://dx.doi.org/10.1002/hyp.10000.
Kilsby, C., Jones, P., Burton, A., Ford, A., Fowler, H., Harpham, C., James, P., Smith, A., Wilby, R., 2007. A daily weather generator for use in climate change studies. Environ. Modell. Software 22 (12), 1705–1719.
Kim, B., Kim, H., Seoh, B., Kim, N., 2007. Impact of climate change on water resources in Yongdam Dam Basin, Korea. Stochastic Environ. Res. Risk Assess. 21 (4), 355–373. http://dx.doi.org/10.1007/s00477-006-0070-5.
Kirchner, J.W., 2006. Getting the right answers for the right reasons: linking measurements, analyses, and models to advance the science of hydrology. Water Resour. Res. 42 (3). http://dx.doi.org/10.1029/2005WR004362.
Klein Tank, A.M.G., Zwiers, F.W., Zhang, X., 2009. Guidelines on Analysis of Extremes in a Changing Climate in Support of Informed Decisions for Adaptation. World Meteorological Organisation.
Klemeš, V., 1986. Operational testing of hydrological simulation models. Hydrol. Sci. J. 31 (1), 13–24.
McMahon, T.A., Peel, M.C., Lowe, L., Srikanthan, R., McVicar, T.R., 2013. Estimating actual, potential, reference crop and pan evaporation using standard meteorological data: a pragmatic synthesis. Hydrol. Earth Syst. Sci. 17 (4), 1331–1363. http://dx.doi.org/10.5194/hess-17-1331-2013.
T.R. McVicar, R.J. Donohue, A.P. O'Grady, L. Li, The effects of climatic changes on plant physiological and catchment ecohydrological processes in the high-rainfall catchments of the Murray-Darling Basin: A scoping study, in: Prepared for the Murray-Darling Basin Authority (MDBA) by the Commonwealth Scientific and Industrial Research Organization (CSIRO) Water for a Healthy Country National Research Flagship, MDBA, Canberra, ACT, Australia, 2010.
Merz, R., Blöschl, G., 2009. A regional analysis of event runoff coefficients with respect to climate and catchment characteristics in Austria. Water Resour. Res. 45 (1). http://dx.doi.org/10.1029/2008WR007163.
Meselhe, E., Habib, E., Oche, O., Gautam, S., 2009. Sensitivity of conceptual and physically based hydrologic models to temporal and spatial rainfall sampling. J. Hydrol. Eng. 14 (7), 711–720. http://dx.doi.org/10.1061/(ASCE)1084-0699(2009) 14:7(711).
Moody, P., Brown, C., 2013. Robustness indicators for evaluation under climate change: application to the upper Great Lakes. Water Resour. Res. 49 (6), 3576–3588.
Müller, M., Kašpar, M., Matschullat, J., 2009. Heavy rains and extreme rainfall-runoff events in Central Europe from 1951 to 2002. Nat. Hazards Earth Syst. Sci. 9 (2), 441–450.
Nazemi, A., Wheater, H.S., 2014. Assessing the vulnerability of water supply to changing streamflow conditions. Eos Trans. Am. Geophys. Union 95 (32). 288-288.
Nazemi, A., Wheater, H.S., Chun, K.P., Elshorbagy, A., 2013. A stochastic reconstruction framework for analysis of water resource system vulnerability to climate-induced changes in river flow regime. Water Resour. Res. 49 (1), 291–305. http://dx.doi.org/10.1029/2012WR012755.
Ndiritu, J.G., Daniell, T.M., 2001. An improved genetic algorithm for rainfall-runoff model calibration and function optimization. Math. Comput. Modell. 33 (6), 695–706. http://dx.doi.org/10.1016/S0895-7177(00)00273-9.
Nossent, J., Elsen, P., Bauwens, W., 2011. Sobol'sensitivity analysis of a complex environmental model. Environ. Modell. Software 26 (12), 1515–1525.
Osidele, O., Beck, M., 2001. Identification of model structure for aquatic ecosystems usingregionalized sensitivity analysis. Water Sci. Technol. 43 (7), 271–278.
Oudin, L., Michel, C., Anctil, F., 2005. Which potential evapotranspiration input for a lumped rainfall-runoff model? Part 1—can rainfall-runoff models effectively handle detailed potential evapotranspiration inputs? J. Hydrol. 303 (1–4), 275–289. http://dx.doi.org/10.1016/j.jhydrol.2004.08.025.
Paton, F., Maier, H., Dandy, G., 2013. Relative magnitudes of sources of uncertainty in assessing climate change impacts on water supply security for the southern Adelaide water supply system. Water Resour. Res. 49 (3), 1643–1667.
Poff, N.L., Brown, C.M., Grantham, T.E., Matthews, J.H., Palmer, M.A., Spence, C.M., Wilby, R.L., Haasnoot, M., Mendoza, G.F., Dominique, K.C., Baeza, A., 2015. Sustainable water management under future uncertainty with eco-engineering decision scaling. Nat. Clim. Change. http://dx.doi.org/10.1038/nclimate2765.
Prudhomme, C., Crooks, S., Kay, A., Reynard, N., 2013. Climate change and river flooding: part 1 classifying the sensitivity of British catchments. Clim. Change 119 (3–4), 933–948. http://dx.doi.org/10.1007/s10584-013-0748-x.
Prudhomme, C., Reynard, N., Crooks, S., 2002. Downscaling of global climate models for flood frequency analysis: where are we now? Hydrol. Processes 16 (6), 1137–1150. http://dx.doi.org/10.1002/hyp.1054.
Prudhomme, C., Sauquet, E., Watts, G., 2015. Low flow response surfaces for drought decision support: a case study from the UK. J. Extreme Events 02 (02), 1550005. http://dx.doi.org/10.1142/s2345737615500050.
Prudhomme, C., Wilby, R.L., Crooks, S., Kay, A.L., Reynard, N.S., 2010. Scenario-neutral approach to climate change impact studies: application to flood risk. J. Hydrol. 390 (3–4), 198–209. http://dx.doi.org/10.1016/j.jhydrol.2010.06.043.
Richardson, C.W., 1981. Stochastic simulation of daily precipitation, temperature, and solar radiation. Water Resour. Res. 17 (1), 182–190.
Saltelli, A., Annoni, P., Azzini, I., Campolongo, F., Ratto, M., Tarantola, S., 2010. Variance based sensitivity analysis of model output. Design and estimator for the total sensitivity index. Comput. Phys. Commun. 181 (2), 259–270. http://dx.doi.org/10.1016/j.cpc.2009.09.018.
Semenov, M.A., 2007. Simulation of extreme weather events by a stochastic weather generator. Clim. Res. 35 (3), 203.
Shafii, M., De Smedt, F., 2009. Multi-objective calibration of a distributed hydrological model (WetSpa) using a genetic algorithm. Hydrol. Earth Syst. Sci. 13 (11), 2137–2149. http://dx.doi.org/10.5194/hess-13-2137-2009.
Sieber, A., Uhlenbrook, S., 2005. Sensitivity analyses of a distributed catchment model to verify the model structure. J. Hydrol. 310 (1–4), 216–235. http://dx.doi.org/10.1016/j.jhydrol.2005.01.004.
Singh, R., Wagener, T., Crane, R., Mann, M.E., Ning, L., 2014. A vulnerability driven approach to identify adverse climate and land use change combinations for critical hydrologic indicator thresholds: application to a watershed in Pennsylvania, USA. Water Resour. Res. 50 (4), 3409–3427. http://dx.doi.org/10.1002/2013WR014988.
Sobol', I.M., Tarantola, S., Gatelli, D., Kucherenko, S.S., Mauntz, W., 2007. Estimating the approximation error when fixing unessential factors in global sensitivity analysis. Reliab. Eng. Syst. Saf. 92 (7), 957–960. http://dx.doi.org/10.1016/j.ress.2006.07.001.
Sorg, A., Bolch, T., Stoffel, M., Solomina, O., Beniston, M., 2012. Climate change impacts on glaciers and runoff in Tien Shan (Central Asia). Nat. Clim. Change 2 (10), 725–731. http://www.nature.com/nclimate/journal/v2/n10/abs/nclimate1592.html#supplementary-information.
Steinschneider, S., Brown, C., 2013. A semiparametric multivariate, multi-site weather generator with low-frequency variability for use in climate risk assessments. Water Resour. Res. http://dx.doi.org/10.1002/wrcr.20528.
Tang, Y., Reed, P., Wagener, T., Van Werkhoven, K., 2007. Comparing sensitivity analysis methods to advance lumped watershed model identification and evaluation. Hydrol. Earth Syst. Sci. Discuss. 11 (2), 793–817.
van der Kamp, G., Hayashi, M., Gallén, D., 2003. Comparing the hydrology of grassed and cultivated catchments in the semi-arid Canadian prairies. Hydrol. Processes 17 (3), 559–575. http://dx.doi.org/10.1002/hyp.1157.
Vano, J.A., Kim, J.B., Rupp, D.E., Mote, P.W., 2015. Selecting climate change scenarios using impact-relevant sensitivities. Geophys. Res. Lett. 42 (13), 5516–5525.
Wagener, T., McIntyre, N., Lees, M.J., Wheater, H.S., Gupta, H.V., 2003. Towards reduced uncertainty in conceptual rainfall-runoff modelling: dynamic identifiability analysis. Hydrol. Processes 17 (2), 455–476. http://dx.doi.org/10.1002/hyp.1135.
Westra, S., Thyer, M., Leonard, M., Kavetski, D., Lambert, M., 2014a. A strategy for diagnosing and interpreting hydrological model nonstationarity. Water Resour. Res. 50 (6), 5090–5113.

S. Westra, M. Thyer, M. Leonard, M. Lambert, Impacts of Climate Change on Surface Water in the Onkaparinga Catchment–Volume 3: Impact of Climate Change on Runoff in the Onkaparinga Catchment. Goyder Institute for Water Research Technical Report Series (14/27), 2014.

Whateley, S., Steinschneider, S., Brown, C., 2014. A climate change range-based method for estimating robustness for water resources supply. Water Resour. Res. 50 (11), 8944–8961.

Wilby, R.L., Dawson, C.W., Murphy, C., O'Connor, P., Hawkins, E., 2014. The statistical downscaling model – decision centric (SDSM-DC): conceptual basis and applications. Clim. Res. 61 (3), 259–276.

Wilcke, R.A.I., Bärring, L., 2016. Selecting regional climate scenarios for impact modelling studies. Environ. Modell. Software 78, 191–201. http://dx.doi.org/10.1016/j.envsoft.2016.01.002.

Zhang, X.Y., Trame, M.N., Lesko, L.J., Schmidt, S., 2015. Sobol sensitivity analysis: a tool to guide the development and evaluation of systems pharmacology models. CPT: Pharmacometrics Syst. Pharmacol. 4 (2), 69–79. http://dx.doi.org/10.1002/psp4.6.